Academic Sciences International Journal of Pharmacy and Pharmaceutical Sciences

ISSN- 0975-1491 Vol 4, Suppl 5, 2012

Research Article

# STRUCTURE BASED DESIGN OF FEW SUBSTITUTED PIPERIDONES AS DIPEPTIDYL PEPTIDASE INHIBITORS

**SOURAV DE[1*], SUBHASIS BANERJEE[1]**

**Department of Pharmaceutical Chemistry, Gupta College of Technological Sciences, Ashram more, Asansol 713301, West Bengal, India. Email: srvmedinipur@gmail.com**

*Received: 18 May 2011, Revised and Accepted: 05 July 2012*

**ABSTRACT**

The incretin based therapies are emerging class of anti-diabetic drugs with two categories viz.; glucagon like peptide-1 (GLP-1) agonists and dipeptidyl peptidase (CD26; DPP-IV) inhibitors. The present work deals with computational ligand docking methodology, AutoDock 4.0 based on Lamarckian genetic algorithm for virtual screens of a series of imidazolyl-(2,6)-diarylpiperidones class of compound of 32 entries for novel and selective inhibitors of the enzyme dipeptidyl peptidase (PDB entry; 2OQI), a potential anti-diabetic drug target. Considering free energy of binding and inhibition constant (KI) as criteria of evaluation, a total of 31 compounds were predicted to be potential inhibitors of dipeptidyl peptidase and 25 compounds displayed greater binding affinities than Sitagliptin, a well-known dipeptidyl peptidase inhibitor. Compound SDM16, 1-(1*H*-imidazol-1-ylacetyl)-2, 6-anthracinyl-3-methylpiperidin-4-one have shown the highest binding energy of -9.08 Kcal/mol with an inhibitory concentration of 0.22μM. Most of the compounds under study have shown significant binding energy as well as interaction in micro molar range. All the comparisons were made with the standard commercially available drug Sitagliptin.

## INTRODUCTION

Docking-based drug design by use of structural biology remains one of the most logical and aesthetically pleasing approaches in drug discovery paradigms. The structured knowledge of the binding capabilities of active site residues to specific groups on the agonist or antagonist leads to proposals for synthesis of very specific agents with a high probability of biological action[1]. Molecular docking is a very popular method employed to investigate molecular association and is particularly useful in the drug discovery arena to study the binding of small molecules (ligands) to macromolecules[2] (receptor). This involves two key components, namely the search algorithm and scoring function; former positions the molecules in orientations and conformations within the active sites, while latter one determining if the orientation chosen by search algorithm is most energetically favorable[3].

Type 2 diabetes is a disease in which the body fails to use insulin properly, combined with relative insulin deficiency. Acute complications include hypoglycemia and diabetic ketoacidosis while long-term complications include cardiovascular disease, chronic renal failure, and retinal damage[4,5]. Injections of insulin provide an effective but inconvenient treatment for the disease. Herein, a treatment involving the indirect control of insulin is described. The incretin hormones GLP-1 and glucose-dependent gastric inhibitory polypeptide (GIP) are released by the small intestine in a response to the intake of food. GLP-1 and GIP both regulate insulin secretion in a glucose-dependent manner. The many roles of GLP-1 within the human body include stimulation of insulin secretion and biosynthesis, inhibition of glucagon release, slowing gastric emptying and reducing appetite. However, the positive effects of endogenous GLP-1 and GIP are limited because they have very short plasma half-lives. The short plasma half-lives are due to rapid enzymatic deactivation. DPP-IV activity is so effective that the half-life of GIP is approximately 7.3 minutes[6] and GLP is a mere 1-2 minutes[7]. The enzyme responsible for the metabolism of these incretin hormones is DPP-IV. By finding efficient inhibitors of DPP-IV the levels of endogenous GLP-1 and GIP can be controlled, thereby providing an effective treatment for type II diabetes. Dipeptidyl peptidase-IV (DPP-IV), also known as ADA and CD26 is an antigenic enzyme expressed on the surface of most cell types and is an intrinsic membrane glycoprotein and a serine exopeptidase which has a preference to cleave X-proline dipeptides at the N-terminus of polypeptides. While substrate specificity studies show DPP-IV's preference for cleavage of peptides containing a proline residue in P1, interestingly, GLP-1 and related glucagon family members contain alanine at this position. DPP-IV plays an important role in glucose metabolism as it is responsible for the degradation of incretins such as glucagon-like peptide 1 (GLP-1)[8]. In an effort to obtain a more complete understanding of the mechanism of inhibition of DPP-IV and to develop potent inhibitors of DPP-IV, computational methods were used to design potential inhibitors. Considering the potentiality of DPP-IV as a promising target in developing oral hypoglycemic candidate, we have virtually designed a series of imidazolyl (2, 6) diarylpiperidone analogs. The rationale behind the design is originated from the fact that the ligand which is attached with the enzyme (Co-crystallized form of DPP-IV obtained from the protein repository) contains piperidone as an important core. A rigorous search algorithm would exhaustively elucidate all possible binding modes between ligand and receptor.

## MATERIALS AND METHODS

### DPP-IV receptor modeling

The receptor model was built by using AutoDock Tools 1.5.1 and MGL Tools 1.5.4 packages (The Scripps Research Institute, Molecular Graphics Laboratory, 10550 North Torrey Pines Road, CA, 92037) running on Linux (Fedora 8). It consists of several steps. First, the 3D crystal structure of DPP-IV (Fig. 1); PDB entry 2OQI[9,10,11] was downloaded from Brookhaven protein data bank and loaded to python molecular viewer. The nonbonded oxygen atoms of waters, present in the crystal structure were removed. After assigning the bond orders, missing hydrogen atoms were added, then the partial atomic charges was calculated using Gasteiger–Marsili method[12]. Non-polar hydrogens were merged, and rotatable bonds were assigned, considering all the amide bonds as non-rotatable. The receptor file was converted to pdbqt format, which is pdb plus ''q'' charges and ''t'' AutoDock type. GLU206 was included as flexible residue for introducing conformational search of flexible side chain. For the same macromolecule was saved in two files: one containing the formatted, flexible GLU206 residue and the other all the rest of the residues in the macromolecule.

### Ligand receptor modeling

**CS ChemDraw 4.5** (Cambridge Soft.Com, 100 Cambridge park drive, Cambridge, MA 02140, USA) was used to draw 2D structures of different ligands. Ligands were further refined and cleaned in 3D by addition of explicit hydrogens by OpenBabel-2.2.1. All the structures were written in pdb file format. AutoDock requires that ligands got partial atomic charges and AutoDock atom types for each atom; it also requires a description of the rotatable bond in the ligand.

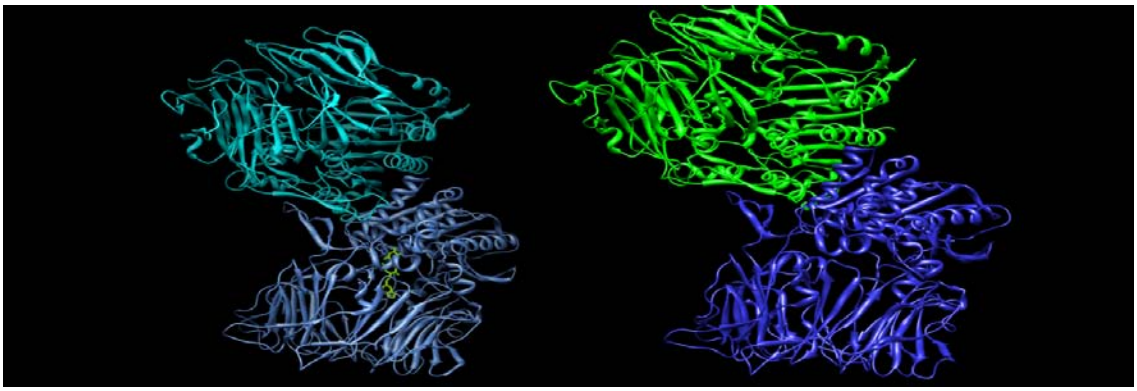

**Fig. 1: Structure of receptor showing A chain(cyan), B chain(cornflower blue), C chain(green) & D chain(Blue)**

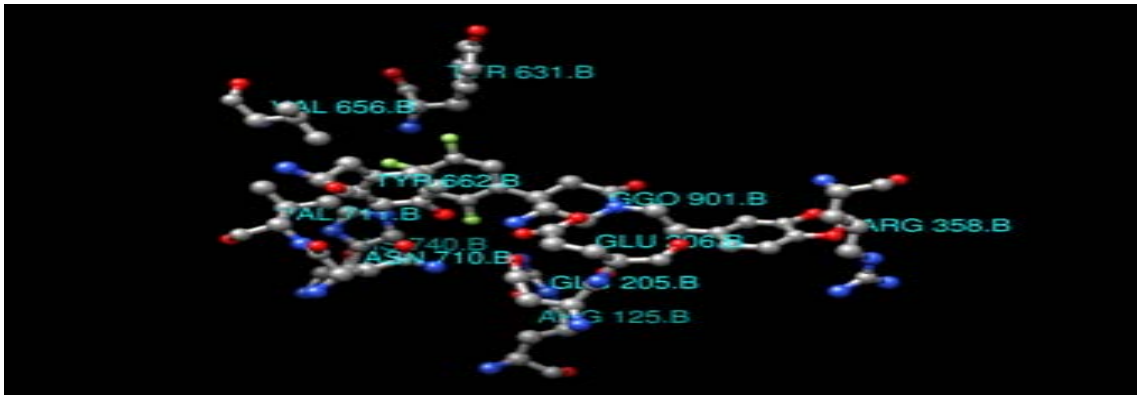


**Fig. 2: Putative active site of DPP-IV residues along with the co-crystallised ligand**

**Molecular docking studies**

AutoGrid 4.0 was introduced to pre-calculate grid maps of interaction energies of various atom types. In all dockings, a grid map with 120*120*120 points, a grid spacing of 0.875 Å (roughly half of the length of a carbon–carbon single bond) were used, and the maps were centered on the macromolecule. In an AutoGrid procedure, the protein is embedded in a 3D grid and a probe atom is placed at each grid point. The energy of interaction of this single atom with the protein is assigned to the grid point. Autodock 4.0 uses these interaction maps to generate ensemble of low energy conformations. For each ligand atom types, the interaction energy between the ligand atom and the receptor is calculated for the entire binding site which is discretized through a grid. This has the advantage that interaction energies do not have to be calculated at each step of the docking process but only looked up in the respective grid maps. Of the three different search algorithms offered by AutoDock 4.0, the Lamarckian Genetic algorithm (LGA) based on the optimization algorithm was used, since preliminary experiments using other two (Simulated annealing and genetic algorithm) showed that they are less efficient, utilizes (discredited) Lamarckian notation that an adaptations of an individual to its environment can be inherited by its offspring. For all dockings, 100 independent runs with step sizes of 0.2 Å for translations and 5 Å for orientations and torsions, an initial population of random individuals with a population size of 150 individuals, a maximum number of $2.5*10^6$ energy evaluations, maximum number of generations of 27,000. AutoDock Tools along with AutoDock 4.0 and Auto Grid 4.0 was used to generate both grid and docking parameter files (i.e., gpf and.dpf files) respectively.

**RESULTS & DISCUSSION**

The results of LGA docking experiments of DPP-IV inhibitors using AutoDock 4.0 and AutoGrid 4.0 are summarized in Table 1. For each docking experiment, the lowest energy docked conformer was selected from 100 runs. The central processing unit for a single docking experiment took 70-90 min, on a 2.19 GHz Intel (R) core2 Duo machine with 3.96 GB of RAM and Linux (FEDORA 2008) operating system. In order to evaluate accuracy of docking, binding energy was used; Inhibition constant (KI) values (μM) were recorded for lowest binding energy mode. 31 molecules showed better inhibition potential than Sitagliptin, **(**3-amino-1-[3-(trifluoromethyl)-5,6-dihydro[1, 2, 4] triazolo [4,3-*a*] pyrazin-7(8*H*)-yl]-4-(2,4,5-trifluorophenyl) butan-1-one**)** , a potent DPP-IV inhibitor, with binding energy -5.4 kcal/mole. The chemical structures of 10 compounds including the reference are shown in the Fig3. Modeling and docking analysis revealed the nature of the active site and some key interactions that enabled the binding of inhibitors to the active site. Among all molecules (32) screened, the docking interactions of 2OQI with SDM16 appeared to be in close proximity and explains the high DPP-IV selectivity. Docking poses and binding interactions of sitagliptin and rest top 10 molecules are shown in Fig.4 and Fig.5 (a-i) respectively. The compounds SDM11 showed hydrogen bonding interactions with the residues VAL341, THR289 respectively, while the compound SDM6 with MET348 and LEU275. The results summarized in Table 1, showed that 11 molecules among the 32 possesses better inhibition potential than the sitagliptin and majority of them were found in close proximity of GLU206.

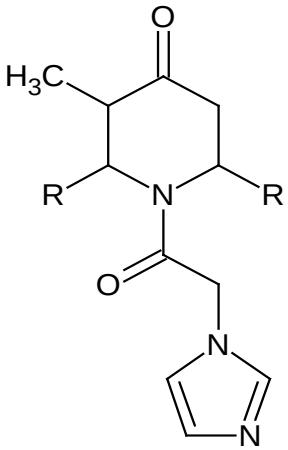

**Table 1: Computationally predicted potencies of all compounds screened**

| S. No. | Compound code | (R) | Binding energy (Kcal/mol) | KI value (μM) | Docking Rank |
|---|---|---|---|---|---|
| 01 | SDM1 | 4-methoxybenzaldehyde | -6.37 | 21.27 | 11 |
| 02 | SDM2 | pentan-2-one | -5.37 | 62.90 | 27 |
| 03 | SDM3 | chloroacetaldehyde | -6.28 | 24.73 | 14 |
| 04 | SDM4 | furan-2-carbaldehyde | -6.26 | 25.62 | 16 |
| 05 | SDM5 | heptanal | -5.22 | 148.17 | 28 |
| 06 | SDM6 | 2-methylpropanal | -5.11 | 180.07 | 30 |
| 07 | SDM7 | 3-methylbutanal | -5.49 | 94.14 | 25 |
| 08 | SDM8 | 3-nitrobenzaldehyde | -5.93 | 44.89 | 22 |
| 09 | SDM9 | 2-hydroxy-5-methoxybenzaldehyde | -6.03 | 38.28 | 19 |
| 10 | SDM10 | furan-3-carbaldehyde | -5.98 | 41.45 | 20 |
| 11 | SDM11 | 5-nitro-1*H*-indole-2-carbaldehyde | -7.56 | 2.89 | 03 |
| 12 | SDM12 | 2-methylthiophene-3-carbaldehyde | -6.61 | 14.19 | 08 |
| 13 | SDM13 | 5-nitro-1*H*-indole-3-carbaldehyde | -6.8 | 9.49 | 06 |
| 14 | SDM14 | 2-hydroxy-5-nitrobenzaldehyde | -5.81 | 55.51 | 24 |
| 15 | SDM15 | 2-hydroxybenzaldehyde | -6.31 | 23.53 | 13 |
| 16 | SDM16 | anthracene-9-carbaldehyde | -9.08 | 0.22 | 01 |
| 17 | SDM17 | pentanedial | -4.45 | 542.05 | 32 |
| 18 | SDM18 | 1*H*-indole-3-carbaldehyde | -6.8 | 10.43 | 07 |
| 19 | SDM19 | benzene-1, 3-dicarbaldehyde | -6.94 | 8.20 | 04 |
| 20 | SDM20 | benzene-1, 2-dicarbaldehyde | -6.28 | 24.98 | 15 |
| 21 | SDM21 | propanal | -4.8 | 301.29 | 31 |
| 22 | SDM22 | pyridine-2-carbaldehyde | -5.9 | 47.66 | 23 |
| 23 | SDM23 | pyridine-4-carbaldehyde | -6.15 | 31.13 | 17 |
| 24 | SDM24 | pyridine-3-carbaldehyde | -6.06 | 36.29 | 18 |
| 25 | SDM25 | 1*H*-pyrrole-2-carbaldehyde | -5.96 | 42.51 | 21 |
| 26 | SDM26 | 2-oxopropanal | -5.12 | 176.27 | 29 |
| 27 | SDM27 | 1, 3-thiazole-2-carboxylic acid | -6.4 | 20.37 | 10 |
| 28 | SDM28 | thiophene-2-carbaldehyde | -6.35 | 21.99 | 12 |
| 29 | SDM29 | thiophene-3-carbaldehyde | -6.53 | 16.40 | 09 |
| 30 | SDM30 | 3, 4-dimethoxybenzaldehyde | -6.9 | 8.77 | 05 |
| 31 | SDM31 | naphthalene-2-carbaldehyde | -8.33 | 667.35 | 02 |
| 32 | ref | SITAGLIPTIN | -5.40 | 109.46 | 26 |

**Potent inhibitors:**

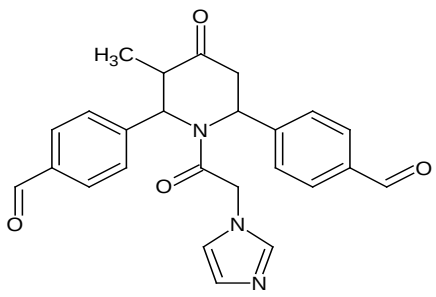

SDM1

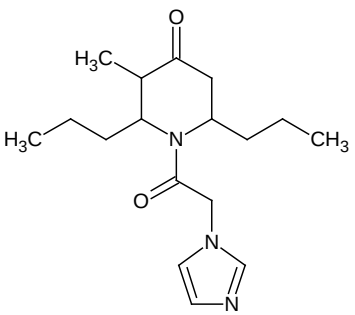

SDM2

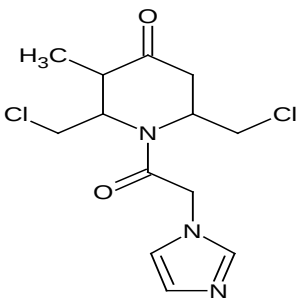

SDM3

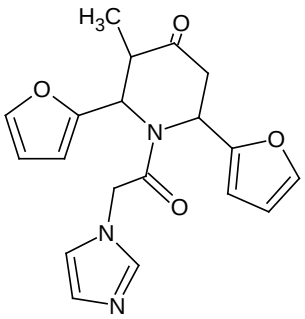

SDM4

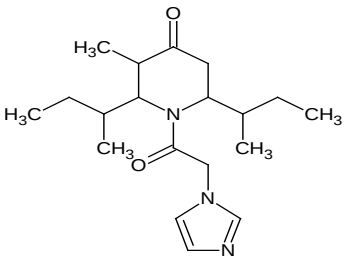

SDM7

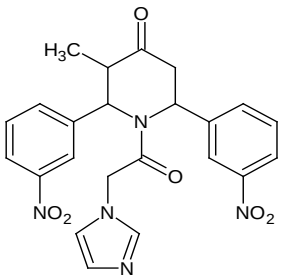

SDM8

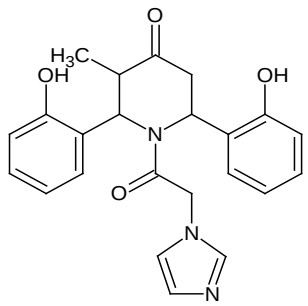

SDM9

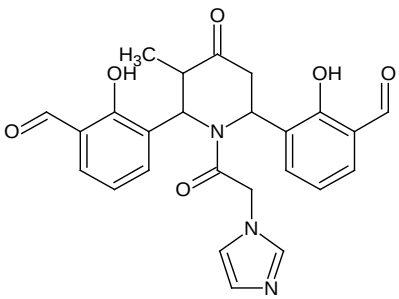

SDM10

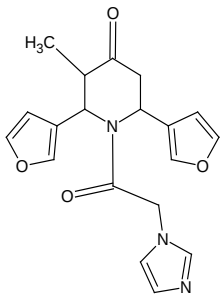

SDM11

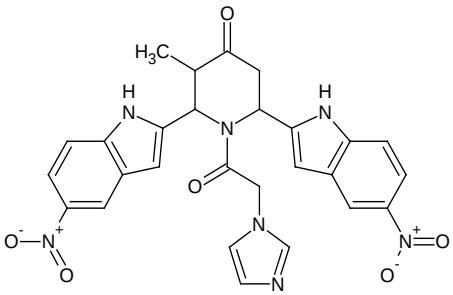

SDM12

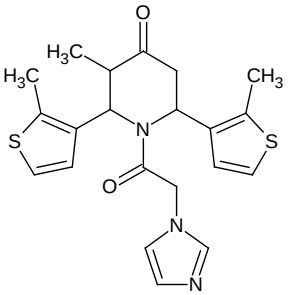

SDM13

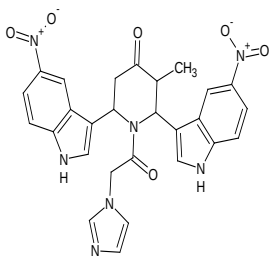

SDM14

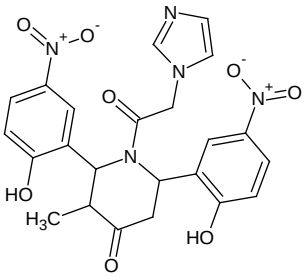

SDM15

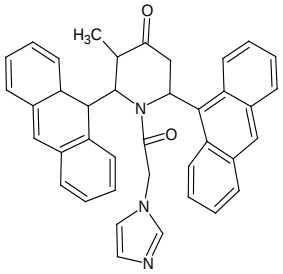

SDM16

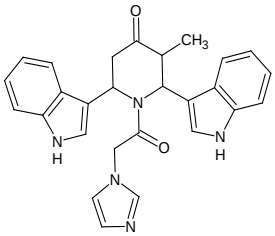

SDM18

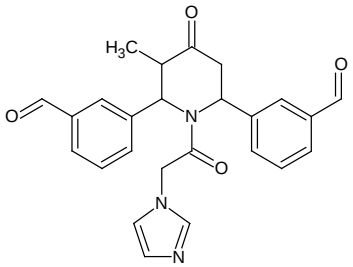

SDM19

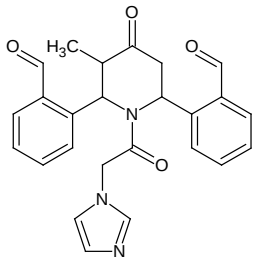

SDM20

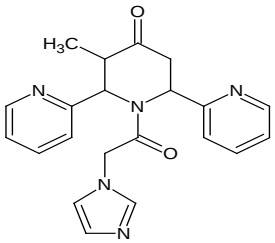

SDM22

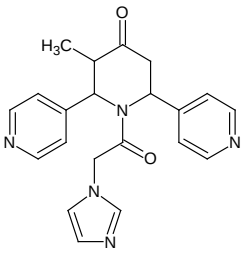

SDM23

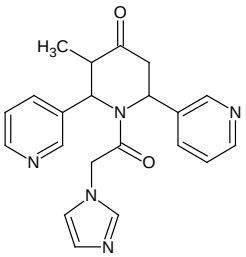

SDM24

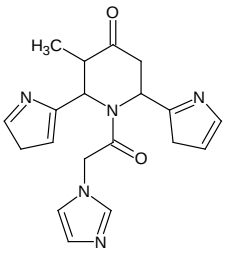

SDM25

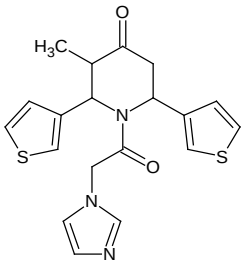

SDM27

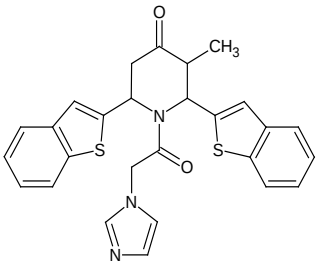

SDM29

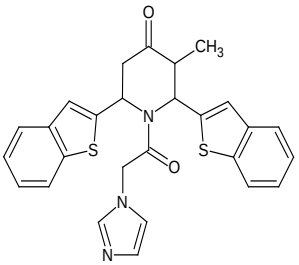

SDM28

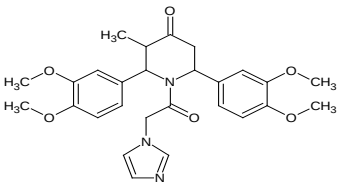

SDM30

**Weak inhibitors**

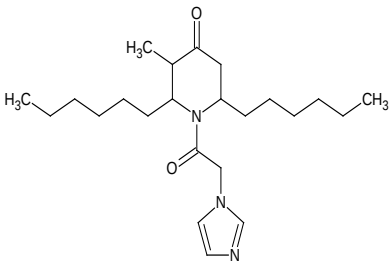

SDM5

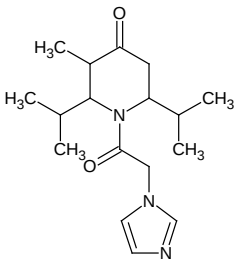

SDM6

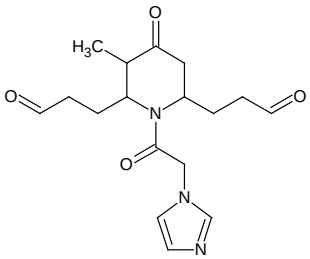

SDM17

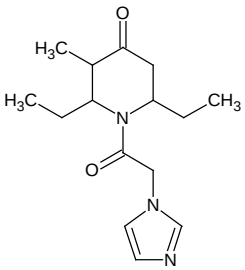

SDM21

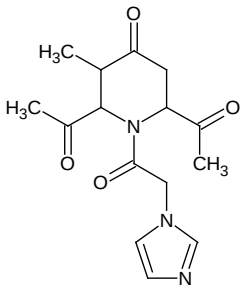

SDM26

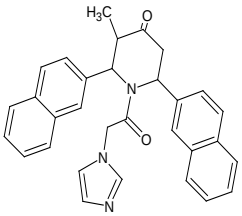

SDM31

**Fig. 3: Chemical structures of the inhibitors under study**

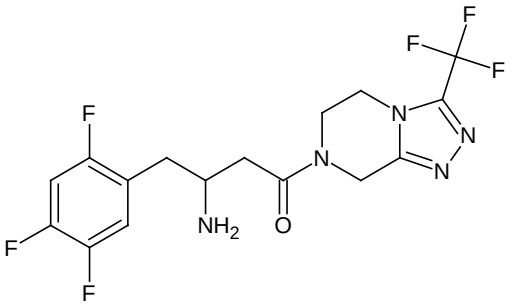

**Sitagliptin (reference)**

This study contributes molecular insight into the binding process, which is of great significance in designing new ligands interfering with DPP-IV and shows a new way of flexible ligand docking program like Auto-Dock, which in turn can produce noncontroversial docking of DPP-IV inhibitors in the enzyme active site.

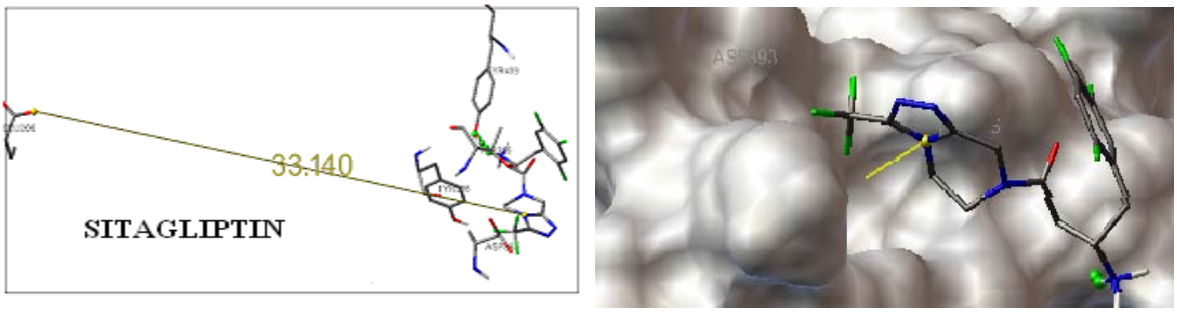


**Stereo view** **Molecular surface view**

**Fig. 4: Binding interaction of Sitagliptin with DPP-IV (PDB ID-2OQI)**

**a.**

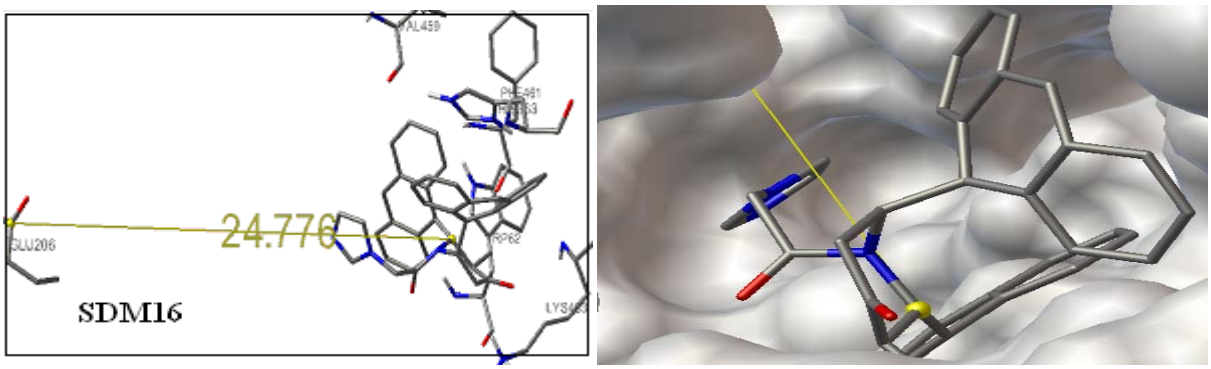


**b.**

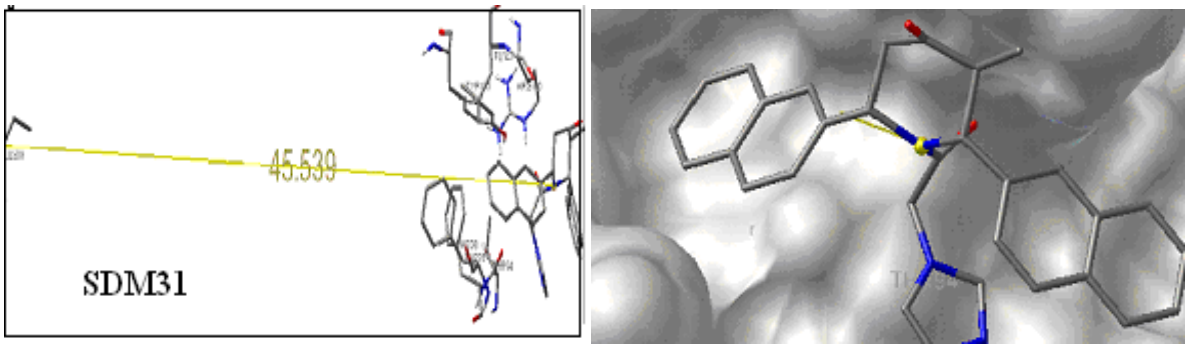


**c.**

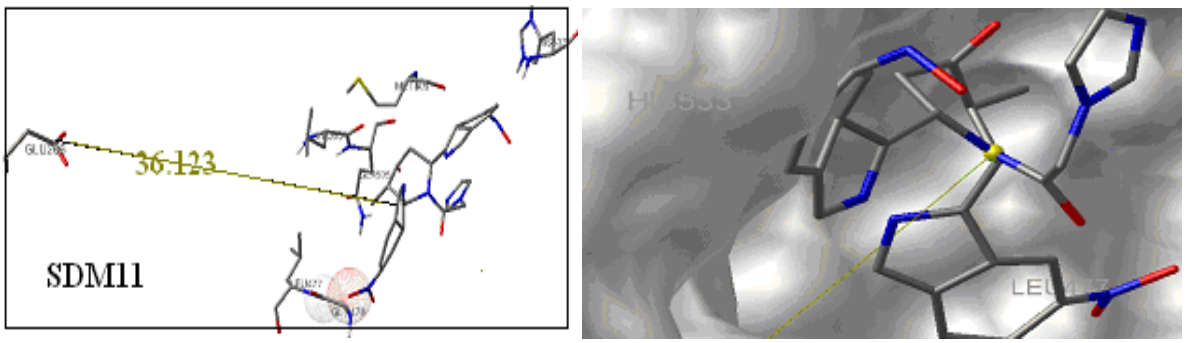


**Fig. 5(a-i): Binding interaction of top ten least energetic molecules with DPP-IV(PDB ID-2OQI)**

**d.**

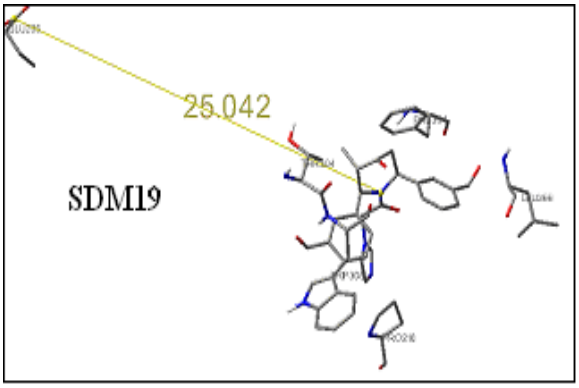


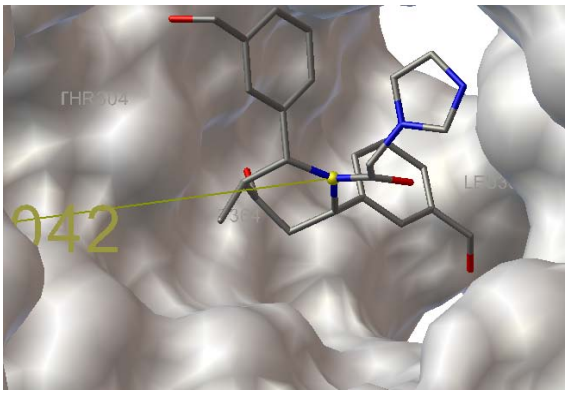

**e.**

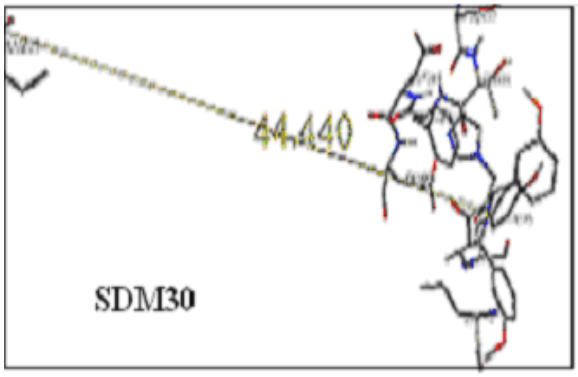


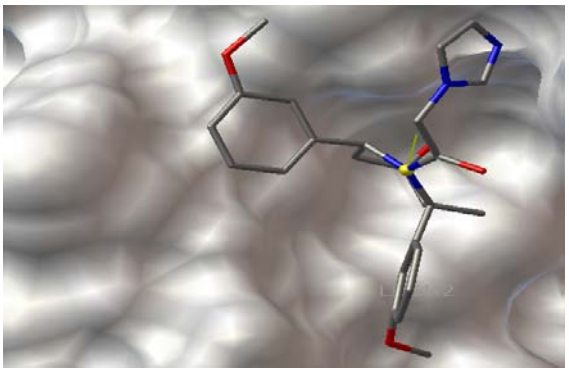

**f.**

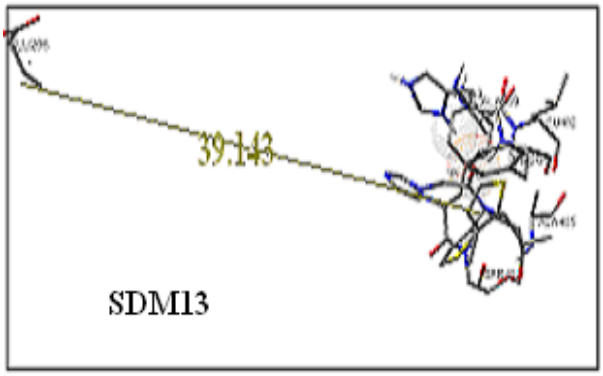


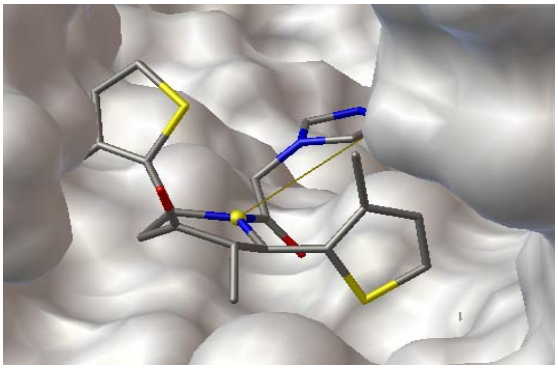

**g.**

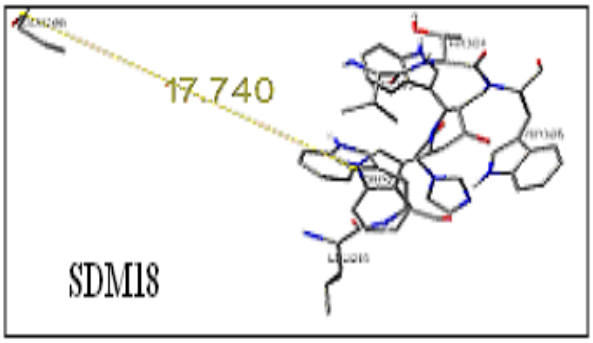


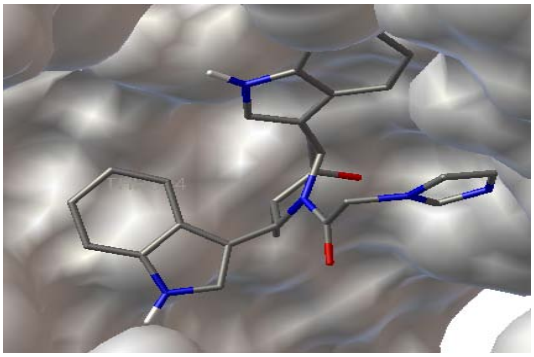

**h.**

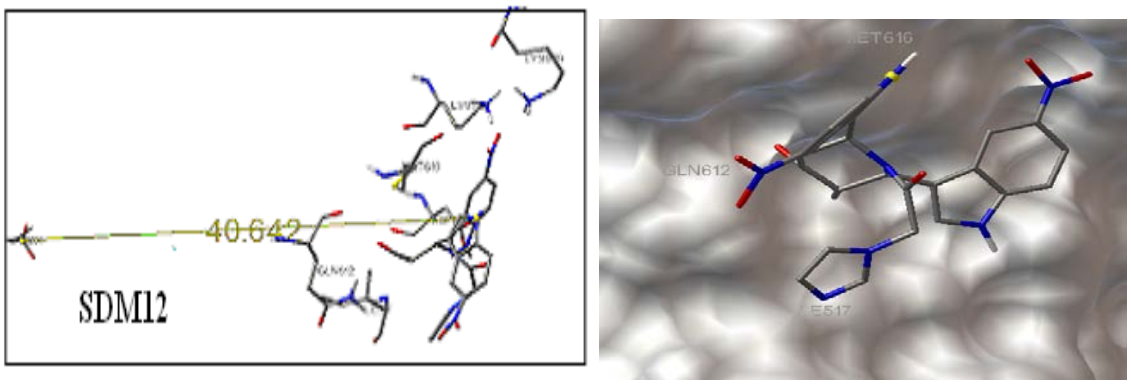


**i.**

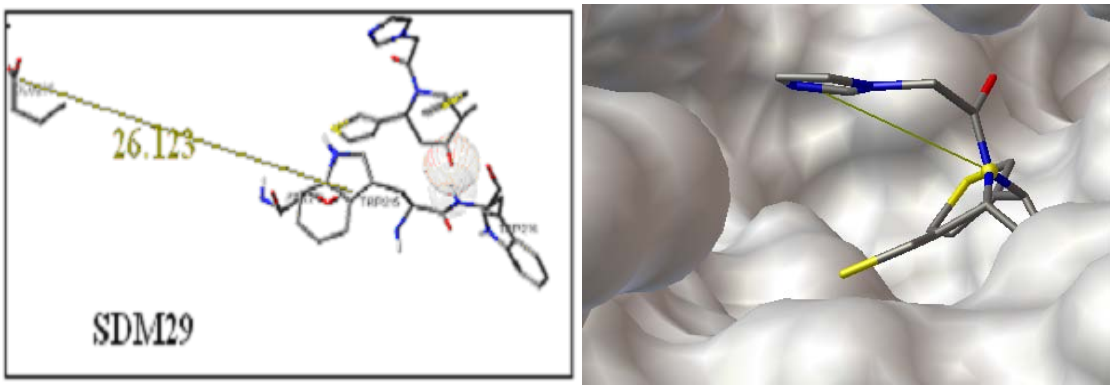


There is a still lot to improve, especially for the empirical binding, free energy force field and KI prediction. The presence of essential pharmacophoric fragments has got a huge value in determining inhibitory activity for DPP-IV. The energy, KI values, and binding interactions revealed from docking poses provide the clues for the design of new molecules thus giving insight on structural requirement for designing much improved analogs.

**ACKNOWLEDGEMENT**

The authors wish to thank Principal, Gupta College of Technological Sciences, Asansol. West Bengal for providing necessary infrastructural and other facilities.

**REFERENCES**

1. Abraham DJ Burger's medicinal chemistry and drug discovery. 6th ed. John Wiley & sons New York; 2003.
2. Barril X, Morley SD Unveiling the full potential of flexible receptor docking using multiple crystallographic structures. J Med Chem 2005;48 :4432–43.
3. Young DC Computational drug design. 1st ed. John Wiley & Sons New York; 2009.
4. Rotella, DP Novel Second-Generation Approaches for the Control of Type 2 Diabetes. J Med Chem 2004;47(17) :4111-12.
5. Weber, A Dipeptidyl Peptidase IV Inhibitors for the Treatment of Diabetes. J Med Chem 2004;47(17) :4135-41.
6. Deacon, CF, Nauck, MA Degradation of Endogenous and Exogenous Gastric Inhibitory Polypeptide in Healthy and in Type 2 Diabetic Subjects as Revealed Using a New Assay for the Intact Peptide. J Clin Endocrinol Metab 2000;85(10) :3575-81.
7. Vilsboll, T Similar Elimination Rates of Glucagon-Like Peptide-1 in Obese Type 2 Diabetic Patients and Healthy Subjects. J Clin Endocrinol Metab 2003;88(1) :220-24.
8. Weber, AE Dipeptidyl Peptidase IV Inhibitors for the Treatment of Diabetes. J Med Chem 2004;47(17) :4135-41.
9. Kwon OS, Park J, Churchich JE Brain 4-aminobutyrate aminotransferase: isolation and sequence of a cDNA encoding the enzyme. J Biol Chem 1992;267 :7215–16.
10. Storici P, Baise DD, Bossa F, Bruno S, Mozzarelli A, Peneff C, Silverman RB, Schirmer T Structure of$\gamma$ -amino butyric acid (GABA) aminotransferase, a pyridoxal 5´-phosphate, and [2Fe-2S] cluster-containing enzyme, complexed with ethynyl- GABA and with the antiepilepsy drug vigabatrin. J Biol Chem 2005;279 :363–73.
11. Toney MD, Pascarella S, Baise DD Active site model for c-amino butyrate aminotransferase explains substrate specificity and inhibitor reactivities. Protein Sci 1995;4 :2226–2374.
12. Gasteiger J, Marsili M Iterative partial equalization of orbital electronegativity-a rapid access to atomic charges. Tetrahedron 1980;36 :3219–28.